

Integrating Network and Attack Graphs for Service-Centric Impact Analysis

Joni Herttuainen^a, Vesa Kuikka, Kimmo K. Kaski

¹Department of Computer Science, Aalto University School of Science, P.O. Box 11000, 00076 Aalto, Finland

Received: date / Accepted: date

Abstract We present a novel methodology for modelling, visualising, and analysing cyber threats, attack paths, as well as their impact on user services in enterprise or infrastructure networks of digital devices and services they provide. Using probabilistic methods to track the propagation of an attack through attack graphs, via the service or application layers, and on physical communication networks, our model enables us to analyse cyber attacks at different levels of detail. Understanding the propagation of an attack within a service among microservices and its spread between different services or application servers could help detect and mitigate it early. We demonstrate that this network-based influence spreading modelling approach enables the evaluation of diverse attack scenarios and the development of protection and mitigation measures, taking into account the criticality of services from the user's perspective. This methodology could also aid security specialists and system administrators in making well-informed decisions regarding risk mitigation strategies.

Keywords Attack graph · Attack modelling technique · Directed acyclic graph · Attack surface · Multilayer network · Lateral movement

1 Introduction

Understanding the nature of cyber threats and protecting systems from attacks has become increasingly critical. Cyberattacks occur when malicious actors compromise the confidentiality, integrity, or availability of computer networks and/or services, by exploiting vulnerabilities therein. [1, 2] Cyber-attackers typically gain

access to computer networks by using a series of exploits, in which each exploit facilitates the next. Once they have an initial entry point, they proceed with lateral movement to spread to the rest of the network and reach other hosts and applications within an organization. [3] This series of exploits constitutes an attack path, while the collection of potential attack paths is an attack graph. [4, 5, 6]

In order to reduce the consequences of these attacks when they occur, there is a need for mitigation strategies to address the vulnerabilities of the computer network. Although perfect security is unattainable, the implementation of defense mechanisms can make systems less susceptible to cyber-targeting. In this, modelling cyber threats and various attack scenarios can serve as a valuable tool in identifying vulnerabilities of the system and consequently deploying protective strategies.

To improve the planning for network security, one needs first to assess the weaknesses in the system. The research presented in [7, 8] introduced a model-based framework and a tool to analyse network security across different architectural scenarios. This framework uses a probabilistic model to represent attack paths and countermeasures, and it enables calculation of the probability of success of the attack based on the specific architectural scenario. A study in [9] investigated strategies for protecting critical resources within enterprise networks, focusing mainly on the use of multiple layers of firewalls. This method deploys a perimeter firewall that separates the corporate network from the Internet, along with internal firewalls for critical subnets.

In the present study, we investigate cyber-attacks using a novel approach that combines network modelling and graphs. [10, 11, 12] This results in an attack graph that is a visual representation of potential paths an attacker could take to compromise a system. [13, 14,

^ae-mail: joni.herttuainen@aalto.fi

15] It describes the structure of attack paths as a directed acyclic graph (DAG) of nodes and links between them. [16] Each node in the attack graph can represent a host, network device, or vulnerability of a network system. [6, 17]

There are two commonly used types of attack graphs. The first one is a directed graph in which nodes denote system states related to security, such as file modifications, levels of user privileges, and trust relationships among hosts. The edges represent possible exploits or actions by the perpetrators. The second type involves nodes that denote the preconditions or postconditions of an exploit, with edges showing the effects of those conditions. Although our primary focus is on directed acyclic attack graphs, our model can also be used to include more general cyclic and recurrent graphs, or causal graphs. [18]

An attack surface of a system refers to the various ways an intruder can exploit its weaknesses to gain access, [13] including resources that a perpetrator can access. The more resources an attacker can access, the larger the attack surface, making the system less secure. To evaluate the security of a system based on its attack surface, several metrics have been developed. [19]

In the present study, we introduce a quantitative attack modelling approach to combine vulnerability metrics of an enterprise network by integrating the attack graph and the structure of the communication network. Our probabilistic approach uses exploitability metrics to evaluate the likelihood that individual vulnerabilities will be exploited along the attack paths. [7, 20] The model estimates the overall probability that a perpetrator successfully gains specific privileges or executes attacks. These probabilities are determined by merging alternative joining attack paths using probability theory for non-exclusive events. [18]

This approach is novel, as it employs a detailed-level network modelling technique [18] that integrates the communication network and attack graph structures. It enables the construction of a quantitative model that describes cyber threats and attacks in the communication network. The outcomes of the model can be presented at varying levels of detail, incorporating attack graph nodes that represent microservices, communication network nodes like servers and network equipment, as well as user services and applications.

Our approach is based on a framework of multilayer network models [21, 22] and allows us to analyse cyber threats and design protective solutions against cyber attacks in enterprise networks. Here, we focus on investigating the infrastructure and communication layer, the cyber attack layer, and the application layer, each of which can be divided into sublayers. With the

present approach, we can also evaluate the operation and robustness of the system from the point of view of physical network, protocol layers, cyber incidents, user services, and applications. All of these layers have the potential to simultaneously exert detrimental impacts on system users. Moreover, we can construct an extra layer for each user service to evaluate metrics related to both incoming and outgoing effects. This in turn allows us to analyse cyber threats targeting specific services or applications as well as the way an attack propagates within a service between microservices. Different services or application servers provide different options for detection, which affects the likelihood of successful mitigation. It is an essential feature of our method that individual attack paths and attack graphs can be extended to different services and servers in the network topology.

In this study, our overarching aim is to create a comprehensive methodology to model how cyber attacks affect user services within an enterprise network architecture. By integrating probabilistic methods to trace attack propagation in attack graphs with user service and application tiers in communication networks, the results of the model help us analyse cyber threats and attacks. Furthermore, microservice vulnerabilities can be linked with user-level service functionalities, which in turn facilitates the design of optimal defense and mitigation strategies. Our model-based approach allows us to explore different cyber attack scenarios and relevant protection strategies against them.

This study is organised such that in Section 2 we discuss related works. Next, in Section 3 we introduce our network-based modelling methodology and related metrics to analyse the impact of cyber attacks. In Section 4 we present the results for impact analysis of cyber attacks against services in a realistic communication network under different scenarios to find ways to mitigate them. Final conclusions are drawn in Section 5.

2 Related Work

In this section, we present a brief overview of related research on modelling cyberattacks and analysing their impact, risk, and resilience in enterprise networks. Here, we focus specifically on graph-based models, attack propagation models, and multilayer network models as well as the metrics to analyse network security. [23, 24, 25] In [24] the authors present a probabilistic metric for network security by aggregating individual vulnerability measures derived from the scores of the Common Vulnerability Scoring System [26, 20] (CVSS) in total network score. The survey on system security metrics presented in [25] proposes a framework to measure

system-level security by using the following four sub-metrics: system vulnerabilities, defense capabilities, attack severity, and situational factors. Here the authors introduce a hierarchical ontology to evaluate relationships among these sub-metrics. They also review existing security metrics and highlight their advantages and limitations to guide the development of more effective security metrics. The study in [27] introduces a set of normalised metrics for comparisons across enterprises. It categorises related metrics into four families (victimization, network size, containment, and topology) that aggregate individual scores into family scores. These metrics are presented through interactive visualisations that show trends over time at individual, family, and overall network levels.

In order to analyse a particular part of the network resilience, we need to apply network modelling techniques and graph models to characterise cyber attacks. [10, 11] The probability formulas that are used to describe connectivity are also useful in explaining the concept of resilience. [28, 29] Here, the connectivity between two nodes is defined as the probability that there is a functioning connection between them. If the connectivity values between all pairs of neighbouring nodes in the network are known, the connectivity probabilities between any pair of nodes in the network can be calculated. [28] This calculation can be performed using either simulation methods or algorithmic techniques. An alternative method to this was introduced in [30], where probabilities were calculated based on spreading probabilities through self-avoiding paths with no repeated nodes.

In the graph-based model of [14], the edge weights indicate potential risks. As a result, an edge with the highest weight represents the worst-case scenario. Depending on the specific problem, the optimal edge or graph can be identified based on the maximum or minimum weight. [14] Another research [31] introduced a host-host model to assess network vulnerabilities and the attack chaining process. This model adopts the point of view of a penetration test to identify the maximum penetration level possible on a host.

In [32] authors consider proactive intrusion prevention and response using attack graphs, dividing them into unconstrained or constrained graphs. Imposing constraints leads to a reduced scope, thus simplifying complexity and improving understanding of potential threats. An unconstrained graph includes all conceivable attack paths without predefined origins or destinations, presuming that the threat source is unidentified and no targeted assets are specified. In contrast, in a constrained graph, particular starting points are defined, including only those paths that are accessible from the origins.

The graph can also end with specified attack goals, concentrating on the protection of critical network assets or the attack surfaces of services or applications employed by users. Several attack surface metrics [13, 33, 34] have been developed to assess an attacker’s capability to compromise a system or its assets.

The enterprise networks are multilayer systems that represent interconnected entities of various types, i.e. networks of nodes, edges, and layers of different types of interactions [22, 35, 36]. To facilitate analysis, multiple methods have been proposed to simplify and contract these networks. The study in [22] presents a comprehensive taxonomy of existing simplification techniques along with the classification of multilayer network methods.

3 Method

In order to derive an attack graph on an enterprise or infrastructure network, we first need to recognise the existing vulnerabilities in its services and how they could be utilized by an attacker. In our model, an attack graph consists of nodes representing the attack states reached by exploiting the vulnerabilities of the system. The vulnerability is denoted by a directed edge (i.e., an attack vector) between two attack states. In addition, the attack graph has certain start and end states, which roughly correspond to an *attacker is ready to attack* and *attacker has reached the desired goal(s)*, respectively.

Our methodology begins with combining the attack graph with the network graph of the underlying communication network in which the services affected by the vulnerabilities are running. This process is shown in Figure 1. Here the attack states on the attack graph are grouped by the affected devices that are represented by nodes in the network graph. As the start and end states do not represent the state of a particular service, they are left out of the grouping. The grouped attack states are then added to the network graph and connected to the corresponding nodes - on which the services are running - with *undirected* edges, as presented in Figure 1b.

The start and end states are connected to the relevant network nodes with *directed* links as shown in Figure 1c. They are only connected to those network nodes that are affected by attack states that are directly connected to the start or end state in the attack graph. The direction of the links is from the start state towards the network and from the network towards the end state. All added directed and undirected links are set to a weight of 1.0, which denotes a probability of 100% connection between the attack states and the nodes to

which they connect. The attack vectors (EN), as represented in the attack graph, are not actually present in the combined graph but are left in Figure 1c with decreased opacity for demonstration purposes.

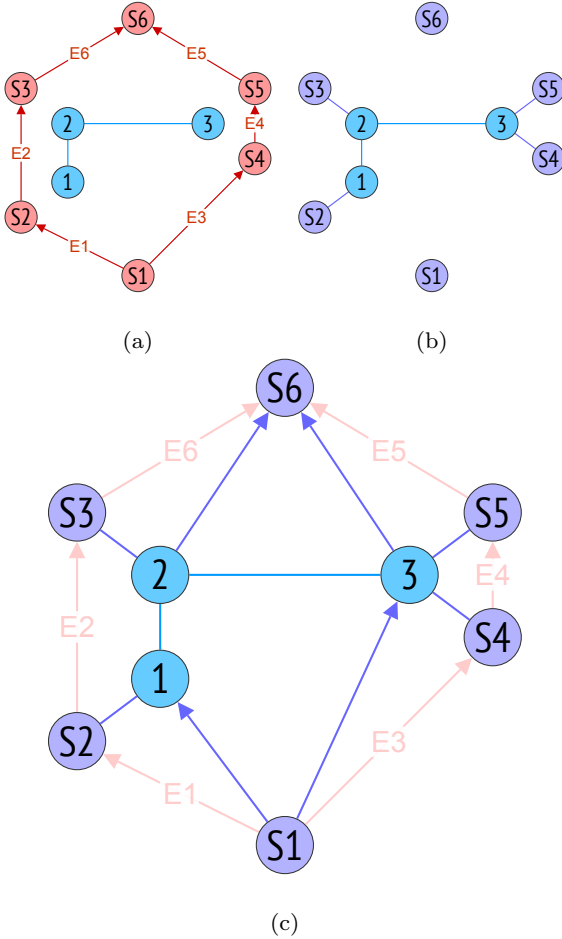


Fig. 1: Combining network graph and attack graph. (Here the graphs are only for demonstrative purpose not the ones used in the rest of the study.) (a) Original network and attack graph in blue and red colour, respectively. (b) Attack states connected to their affected services. (c) Combined graph with connected start and end states $S1$ and $S6$, respectively.

The network graph link weights (w_n) can be interpreted to represent, e.g., the probabilities of working routing between the nodes, the probabilities of the attack passing the network intrusion detector or a combination of different probabilities. For the purposes of demonstrating our model, we assume that the network-level probabilities are aggregated into single values and that the pairwise node-to-node probabilities are equal in both directions, although neither is a restriction of the model.

Our analysis of an attack is based on both the attack graph and the combined graph. While the attack graph can be used for the analysis of exploitability and impact of an attack, the combined graph takes into account the possibility of the attack at the network level. For example, in Figure 1a there are two possible attack paths: $(E1, E2, E6)$ and $(E3, E4, E5)$. If for any reason the service in node 2 is unreachable from node 1, the former attack path is no longer possible. This can be clearly seen in the combined graph in Figure 1c: the attack vector $E2$ cannot be exploited if node 2 and, thus, the attack state $S3$ is unreachable from $S2$. However, the other attack path traversing through the service in node 3 is still possible as it is independent of the service in node 2.

Using the combined graph, we calculate the probabilities of each attack vector EN present in the attack graph at the network level. That is, for each attack step $S_i \rightarrow S_j$, the corresponding network-level probability (p_N) of reaching the target attack state from the source attack state via any non-intersecting path through the network is calculated using the Simple Contagion Algorithm presented in [37]. The combined probability of a successful exploitation of an attack vector between two states is then calculated as the product of the probability that the attack step passes the underlying network and the probability of the vulnerability being exploited:

$$p(i, j) = p_N(i, j) * p_E(i, j). \quad (1)$$

Here, p_N and p_E are the probability of an attack from state i to state j passing through the network and the exploitability of the vulnerability connecting the states (as depicted in the attack graph), respectively. Since the attack states are connected to the network nodes with links of weight 1.0, regardless of the network link weights w_n , the network-level probability of a connection between the states is equal to the probability of a connection between their corresponding nodes. That is:

$$\forall i \in G_m, j \in G_n : p_N(i, j) = p_N(m, n),$$

where i and j are the source and target attack states and G_m and G_n are sets consisting of attack states grouped to services running on nodes m and n in the network, respectively. Moreover, since the attack can traverse any non-intersecting path through the network, if $w_n < 1$, the more possible paths there are between the states, the larger the p_N is.

In order to measure the importance of different vulnerabilities and services, we use metrics based on the probability, expected impact, and expected cumulative

impact of an attack. Our interpretation and calculations of the probabilities of different states in the attack graph are based on the principles presented in [20]. First of all, our model assumes that the probability of a vulnerability being exploited (i.e., exploitability) represents the probability that an attack vector will be exploited during an attack. Secondly, we assume that a vulnerability can only be exploited if the attack has already propagated to the preceding state. Thirdly, our model considers the different paths leading to a state disjunctive, which means that the probability of an attack reaching a state is equal to the probability that at least one of the attack paths leading to the state is traversed during an attack.

The overall probability of a single attack vector being successfully exploited during an attack is calculated as:

$$P(i, j) = P(i) * p(i, j),$$

where $p(i, j)$ is the probability of a vulnerability between states i and j being successfully exploited (see: Eq. 1) and $P(i)$ is the probability that an attack has reached the state i . Since the different paths leading to a state are considered disjunctive, $P(i)$ is calculated as:

$$P(i) = 1 - \prod_{j \in A} [1 - P(j, i)],$$

where A is a set of all states immediately preceding state i .

Our calculation of expected impact is based on the expectation from probability theory:

$$\text{ExpectedImpact} = \text{Probability} * \text{Impact},$$

which is motivated by the calculation of risk as a function of likelihood and severity in [14] and assessment of risk as a combination of likelihood and impact in [38]. The impact is a property of the vulnerabilities (attack vectors) between the attack states and not of the attack states themselves. Furthermore, the impact values of the different attack vectors leading to a state may differ from each other. To account for this, we consider the expected impact $E[I_i]$ of reaching a state as a sum of the expected impacts of the attack vectors $E[I_{j,i}]$ leading to the state i :

$$E[I_i] = \sum_{j \in A} E[I_{j,i}] = \sum_{j \in A} P(j, i) * I(j, i), \quad (2)$$

where $I(j, i)$ is the impact of an attack vector from state j to state i and A is the set of all states j immediately preceding the state i . Now we can calculate the expected cumulative impact of an attack reaching a certain state:

$$CE[I_i] = E[I_i] + \sum_{j \in B} E[I_j], \quad (3)$$

where B is the set of all the states on every possible path from the beginning of an attack to state i , excluding the state i itself.

Next we calculate three other metrics that are motivated by the grouping of attack states in their affected services, namely expected cumulative inbound and outbound impacts, as well as expected node-wise impact. The expected cumulative inbound impact represents the case in which the attack has propagated to a certain service and gained a foothold there but has not yet propagated further within the service. It is calculated as a sum of the expected impacts of all the preceding states and the expected impacts (see: Eq. 2) of the incoming attack vectors to the service:

$$C_{IN}(n) = \sum_{i \in C} (E[I_i] + \sum_{j \in G_n} E[I_{i,j}]), \quad (4)$$

where C is the set of all states on every possible path from the beginning of an attack to the states in G_n , excluding the states in G_n , which is the set of attack states grouped by the service running on node n . The expected cumulative outbound impact can be calculated by extending C_{IN} :

$$C_{OUT}(n) = C_{IN}(n) + \sum_{\substack{i \in G_n \\ j \in D}} E[I_{i,j}], \quad (5)$$

where D is the set of all states immediately following any state in G_n , including those in G_n , which is the set of attack states grouped by the service n . This represents the case in which a service is used to gain a foothold in another service or to fulfill the criteria set for a successful attack (i.e., to reach the end state).

The node-wise impact represents the maximum impact that can be caused to a single service if all the attack vectors of the service are exploited. It is calculated as a sum of the expected impacts of attack vectors affecting a particular node without taking into account the impact cumulated prior to the attack reaching the service:

$$C_{NODE}(n) = \sum_{i \in G_n} E[I_i], \quad (6)$$

where G_n is the set of attack states grouped to service n .

An illustrative example of the attack vectors and states that are included in each of the metrics is presented in Appendix A.

4 Results

In order to make our experimental cyberattack case realistic, we chose a network representing what used to be a real-world infrastructure network, shown in the bottom layer in Figure 2. To simulate possible attacks on the services of this network, we used a realistic attack graph that represents vulnerabilities found in a multi-cloud enterprise network originally presented in [14]. To combine the attack graph with the network graph, as a first step, we group the attack states by the affected services as presented in [14]. For each of the services, we selected a representative node in the network graph. The grouping of vulnerabilities in services and the grouping of services to the selected network nodes is listed in Table 1 and shown in the top layer in Figure 2.

The attack graph, as well as the grouped network nodes, are depicted in Figure 3. It consists of 18 states (start, end and 16 attack states), 9 possible attack paths from start to end, and a total of 14 distinct exploitable vulnerabilities. Each vulnerability is represented by one or several directed edges in the attack graph and has both an impact value and an exploitability value calculated using CVSS. The computational methodology for these values is presented in [39] and follows the guidelines shown in [26]. The list of vulnerabilities, their impact values, exploitability, and their corresponding attack vectors in the attack graph can be seen in Table 2.

Network Service	Node N:o	Attack States
NAT Server	1	S7, S8
VM Groups	2	S9, S10, S11, S12
Database	3	S3, S4
Web Server	4	S13, S14, S15
Workstation	6	S16, S17
Admin Server	7	S2
Mail Server	8	S5, S6

Table 1: Grouping attack states by their affected services.

4.1 Initial results

In our initial analysis, we set all network link weights to $w_n = 1.0$ denoting a 100% probability that a communication or an attack will succeed at the network level. This is effectively the same as only considering the attack graph without there being any defense mechanisms present in the network preventing the attack.

This is done to get an understanding of how the different cumulative metrics behave without, yet, taking the network into account.

In Figure 4, we present the node-wise impact C_{NODE} for all affected services (nodes). Here, it is clearly seen that the expected impacts of the vulnerabilities that affect node 2 sum up to be the biggest concern in the attack graph. This is not surprising, since the service in node 2 has the biggest attack surface, i.e., the most attack vectors provide a foothold to the node and thus the probability of successfully attacking this node is expected to be high. The second explaining factor is that the service in node 2 has the largest overall number of attack vectors, so there is a possibility of a higher impact to begin with even if we take into account that it has the least exploitable attack vectors $E3$, $E4$, and $E20$ as seen in Tables 1 and 2. The C_{NODE} values of the rest of the nodes seem to be consistent with this reasoning, as nodes 1, 3, and 7 have the next highest number of affecting attack vectors and the next largest attack surfaces, which is indicated by their high C_{NODE} values, whereas $C_{NODE}(6)$ and $C_{NODE}(8)$ are significantly lower. The low $C_{NODE}(4)$ value, although more attack vectors affect node 4 than node 8, can be explained by the fact that the attack vector $E2$ does not have an impact.

The results for the expected cumulative impact of each of the attack states ($CE[I]$, see Eq. 3) are shown in Figure 5a. As expected, the latter states of the attack score higher than the earlier states of the attack (e.g., $CE[I_{S11}] > CE[I_{S15}]$ and $CE[I_{S3}] > CE[I_{S15}]$) and the cumulation of expected impact within a service can be witnessed (e.g., $CE[I_{S12}] < CE[I_{S10}] < CE[I_{S9}]$). In particular, $S2$ has a very high expected cumulative impact due to many attack paths consisting of attack vectors with both high exploitability and a high impact leading to it. Note that at the beginning of an attack ($S1$), there is no cumulative impact ($CE[I_{S1}] = 0$) since the attack has not yet started. Furthermore, since the attack states $S14$ and $S17$ are only reached from $S1$ by exploiting vulnerabilities that do not have impact ($E2$ and $E1$, respectively), the expected cumulative impact of reaching these states is also nonexistent. Since $S18$ is the state in which an attacker reaches its objectives, $CE[I_{S18}]$ denotes the expected cumulative impact of a successful attack ($S1 \rightarrow S18$). As all the attack paths lead to $S18$, this value consists of the expected cumulated impact of all the attack paths, and therefore the score is higher than for the rest of the attack states. Logically, the cumulative impact is highest at the end of an attack.

A similar trend is reflected in the expected cumulative inbound (C_{IN} , Eq. 4) and cumulative outbound

Vulnerability	Exploitability / 10	Impact	Attack Vector(s)
MALICIOUS-WEBSITE	1.0	0.0	E1
DIRECT-ACCESS	1.0	0.0	E2
CVE-2010-3847	0.339258	10.00085	E3, E4, E20
CVE-2003-0693	0.99968	10.00085	E5, E6
CVE-2007-4752	0.99968	6.442977	E7
CVE-2001-0439	0.99968	6.442977	E8
CVE-2008-4050	0.85888	10.00085	E9, E10
CVE-2008-0015	0.85888	10.00085	E11, E12, E21, E22, E23
CVE-2009-1918	0.99968	10.00085	E13, E16
CVE-2018-7841	0.99968	6.442977	E14, E18
CVE-2004-0840	0.99968	10.00085	E15
CVE-2008-5416	0.7952	10.00085	E17, E19
CVE-2001-1030	0.99968	6.442977	E24
CVE-2009-1535	0.99968	6.442977	E25

Table 2: Vulnerabilities present in the attack graph. The exploitability and impact values are calculated based on the CVSS scores. [26] Originally presented in [39].

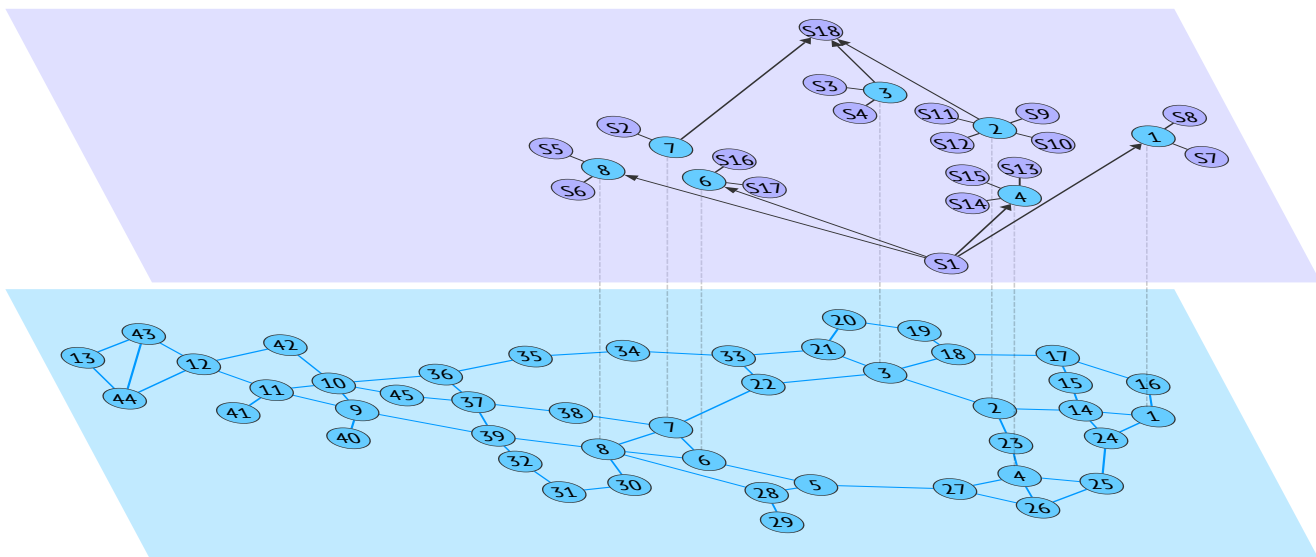


Fig. 2: The combined graph used in the experiments. The bottom layer represents the original communication network graph and the top layer represents the attached attack states connected to the relevant nodes of the network.

(C_{OUT} , Eq. 5) impact metrics as can be seen in Figures 5b and 5c, respectively. Measured by C_{IN} , the nodes 1, 4, 6 and 8, which provide a foothold in the network, score lower than the nodes further down on the attack path. This is also the general trend with C_{OUT} , with the exception of node 1, since clearly $C_{OUT}(3)$ is less than $C_{OUT}(1)$. If we consider these measures to reflect on how large the overall impact is if a node is *attacked* (C_{IN}) and *used to attack other services* (C_{OUT}), the reasoning for this is straightforward, since there is only one outbound attack vector that can be exploited

from node 3 while there are three of those that can be exploited from node 1.

What is most noticeable are the very high $C_{IN}(7)$ and $C_{OUT}(7)$ values, even though node 7 has one of the smallest C_{NODE} values. This, again, is due to the nature of the metrics used here. That is, while an attack to the node itself might not be of high concern as it has a low impact, the fact that the attack has propagated that far should be alarming, as the attack has, with a high probability, propagated through services that cause the attack to have a high impact. Note

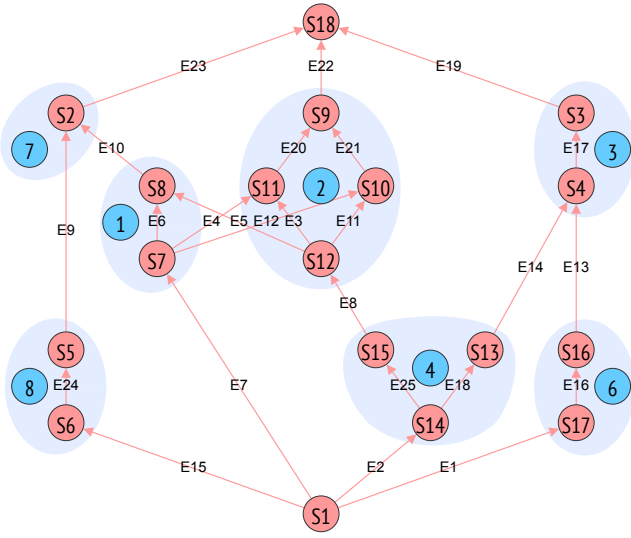


Fig. 3: Attack graph used in the experiments with the states grouped by affected services. $S1$ and $S18$ are the start and end states, respectively.

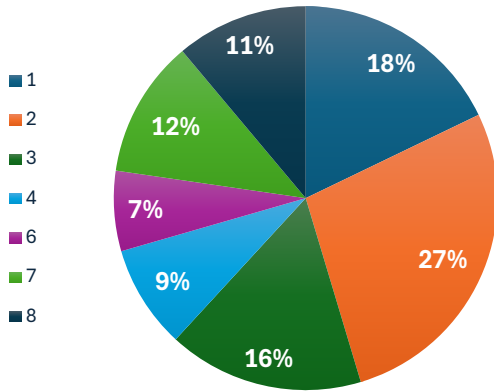


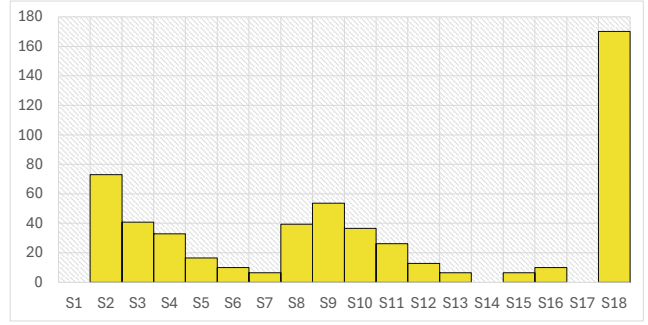
Fig. 4: Initial node-wise impact, C_{NODE} , per node n .

that $C_{IN}(4) = 0$ and $C_{IN}(6) = 0$ are special cases due to the fact that the attack vectors $E1$ and $E2$ have no impact.

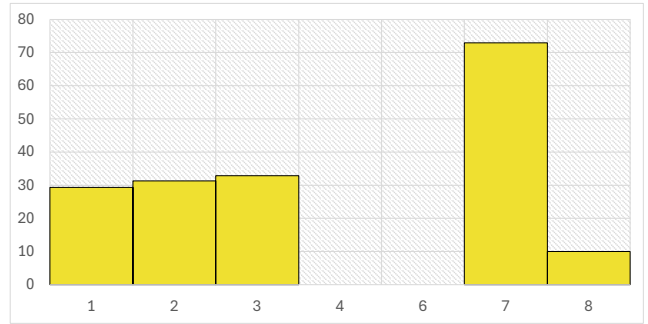
4.2 Mitigation of individual vulnerabilities

In enterprise networks with vulnerabilities of varying degrees, it is important to understand the impact of each vulnerability to be mitigated or fixed. In an attack graph, fixing a vulnerability can be simulated by setting the exploitability of the affected attack vectors to zero ($p_E = 0.0$).

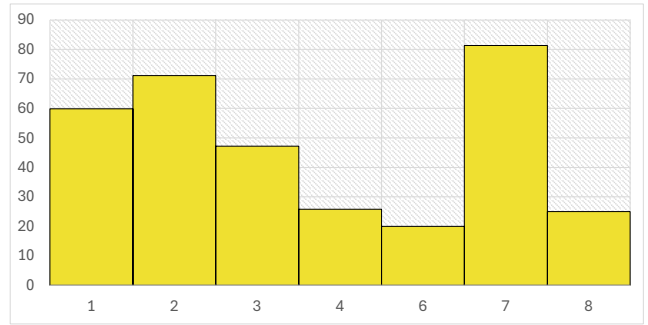
To demonstrate the usefulness of the model in analysing the impact of a single vulnerability on the attack, we perform a series of calculations, each after having simulated fixing one vulnerability. In each simulation run, we



(a)



(b)



(c)

Fig. 5: Initial results for expected cumulative impact (vertical axis) across different metrics. (a) $CE[I_i]$, expected cumulative impact per attack state (Eq. 3). (b) $C_{IN}(n)$, expected cumulative inbound impact per node (Eq. 4). (c) $C_{OUT}(n)$, expected cumulative outbound impact per node (Eq. 5).

calculate the C_{IN} , C_{OUT} and $CE[I_{S18}]$ after fixing one of the vulnerabilities and compare the results with those of the original attack graph. Here, the change signifies how much the expected cumulative impact changes on existing attack paths from the beginning of an attack ($S1$) to the relevant attack states. Since fixing a vulnerability results in at least one attack path having an attack vector with zero exploitability ($p_E = 0.0$), thus

making the path infeasible, the impact is calculated only for the portion of the path that remains feasible.

Figure 6 depicts the relative changes of node-wise expected cumulative inbound impacts (C_{IN}) as well as their averages after mitigating a vulnerability. Intuitively, one could assume that fixing the vulnerabilities that work as entry points into the network would have the biggest effect on the cumulative impact, as fixing these vulnerabilities often makes multiple attack paths impossible. This intuition is mainly supported by our results, as fixing foothold vulnerabilities seems to have the largest overall effect on C_{IN} . For example, *DIRECT-ACCESS* has, on average, the highest relative change as measured by C_{IN} , whereas vulnerabilities that are exploited later in the attack, such as *CVE-2018-7841*, have a significantly lower relative change. Since initially both $C_{IN}(4) = 0$ and $C_{IN}(6) = 0$, the relative change is also zero for these nodes, even when it is impossible to attack them after fixing the vulnerabilities that provide a foothold in these nodes.

In some cases, fixing a vulnerability in the early stages of the attack completely eliminates all C_{IN} for a certain node, while in other cases several vulnerabilities need to be fixed to fully mitigate all C_{IN} to a node. For example, by mitigating *CVE-2004-0840*, all $C_{IN}(8)$ is eliminated, but achieving the same for node 2 requires fixing both *CVE-2007-4752* and *CVE-2009-1535*.

Since we measure the change of cumulative impact on the full existing attack path, we can see that fixing a vulnerability does not, in general, fix the whole attack path to a node. However, the earlier the attack path is mitigated, the bigger the change in cumulated impact. In Figure 6, this effect can be seen by examining the relative change of $C_{IN}(1)$ on the attack path consisting of vulnerabilities *CVE-2009-1535*, *CVE-2001-0439* and *CVE-2003-0693* (*E25-E8-E5* in Figure 3). Clearly, the change is larger if *CVE-2009-1535* is mitigated instead of *CVE-2003-0693*.

The relative change in the expected cumulative outbound impact (C_{OUT}) can be seen in Figure 6. These results are consistent with those of the C_{IN} case. That is, fixing vulnerabilities in the early states of the attack path has a larger change than fixing vulnerabilities in the later states. Also, as expected, vulnerability *CVE-2009-1535* is one of the most significant ones, as it is part of several attack paths with a high expected cumulative impact.

The noticeable difference from the C_{IN} case is the presence of change in nodes 4 and 6. As mentioned above, removing the vulnerabilities that provide a foothold to these nodes would make it impossible to attack them. This can be seen in figure 7 by looking at the relative change of $C_{OUT}(4)$ and $C_{OUT}(6)$ when fixing vulnera-

bilities *DIRECT-ACCESS* and *MALICIOUS-WEBSITE*, respectively.

Similarly to the C_{IN} case, fixing *CVE-2004-0840* mitigates all $C_{OUT}(8)$ and fixing both *CVE-2007-4752* and *CVE-2009-1535* would eliminate all $C_{OUT}(2)$. Although the former can be directly interpreted on the basis of Figure 7, the latter can not, as the relative changes of $C_{OUT}(2)$ after fixing those two vulnerabilities do not sum up to -1 . This is due to the fact that while fixing *CVE-2007-4752* blocks all attack paths targeting node 2 through node 1 and fixing *CVE-2009-1535* blocks those that pass through node 4, preventing the attack from progressing through node 2 requires fixing both of them.

The relative change in the expected cumulative impact ($CE[I_{S18}]$) of a successful attack ($S1 \rightarrow S18$) can be seen in Figure 8. In line with the previous findings, fixing vulnerabilities in earlier states has a high relative change. Especially, *DIRECT-ACCESS* is clearly the most impactful vulnerability. In addition and consistent with previous findings, fixing *CVE-2009-1535* results in a high relative change of $CE[I_{S18}]$. An interesting finding is that the vulnerability with the second highest relative change is *CVE-2008-0015*, which is not an entry-point attack vector and does not have a high relative change as measured by C_{IN} or C_{OUT} . One reason for this is the high impact and high exploitability of the vulnerability. However, the main reason is the number of attack paths that exploit this vulnerability, which can be seen by locating the numerous attack vectors of the vulnerability (Table 2) on the attack graph (Figure 3).

4.3 Securing individual nodes

Fixing a vulnerability completely is not always possible for various reasons. For example, in our scenario, one exploitable vulnerability that cannot be fully fixed is "user browsing a malicious web page". As a more general example, there may not be a patch available for the vulnerability or the patch cannot be applied due to incompatibility issues with other systems or due to it causing downtime in operational systems. In these cases, mitigation strategies include other security measures, such as implementing monitoring solutions to help detect suspicious activity. These measures may not completely stop the attack, but they decrease the probability of a successful attack.

To investigate added monitoring as a mitigation measure, we perform another series of calculations, each time decreasing the probability of a successful attack to or from a node. This is done by reducing the exploitability of the known vulnerabilities of the service running

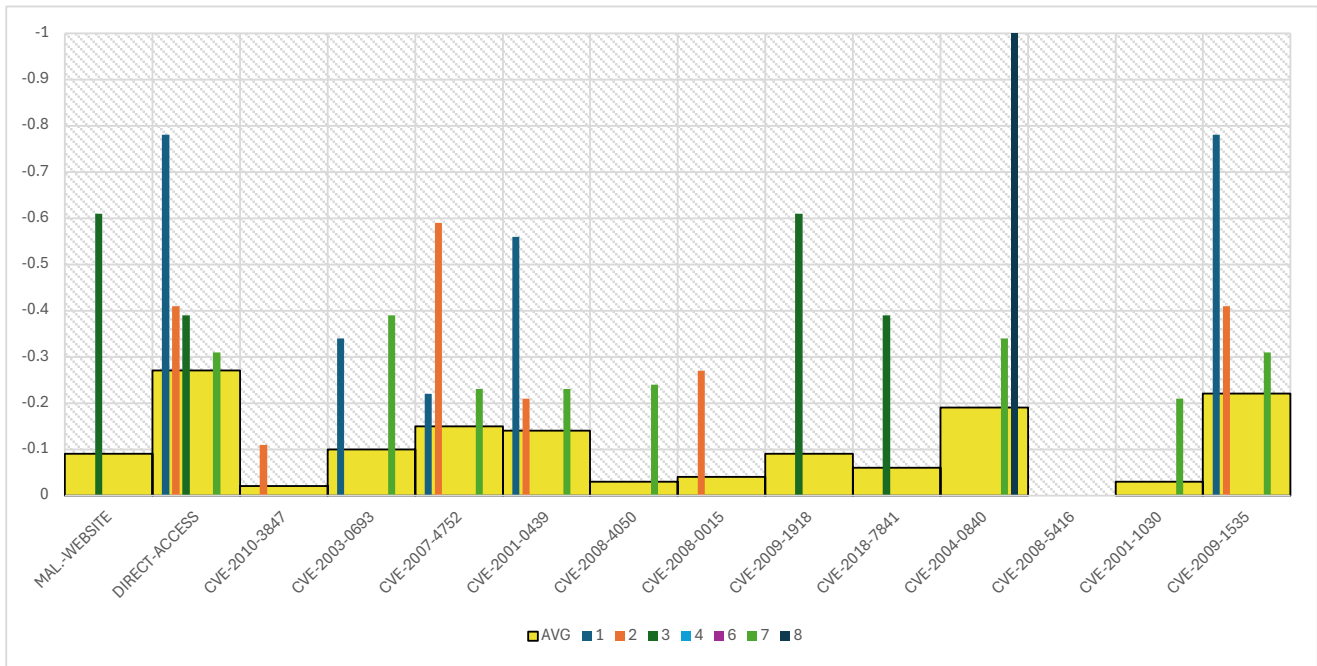


Fig. 6: Relative change in the node-wise expected cumulative inbound impact, C_{IN} , after fixing a vulnerability. The individual bars represent the relative change of C_{IN} per node n . Note the reversed vertical axis.

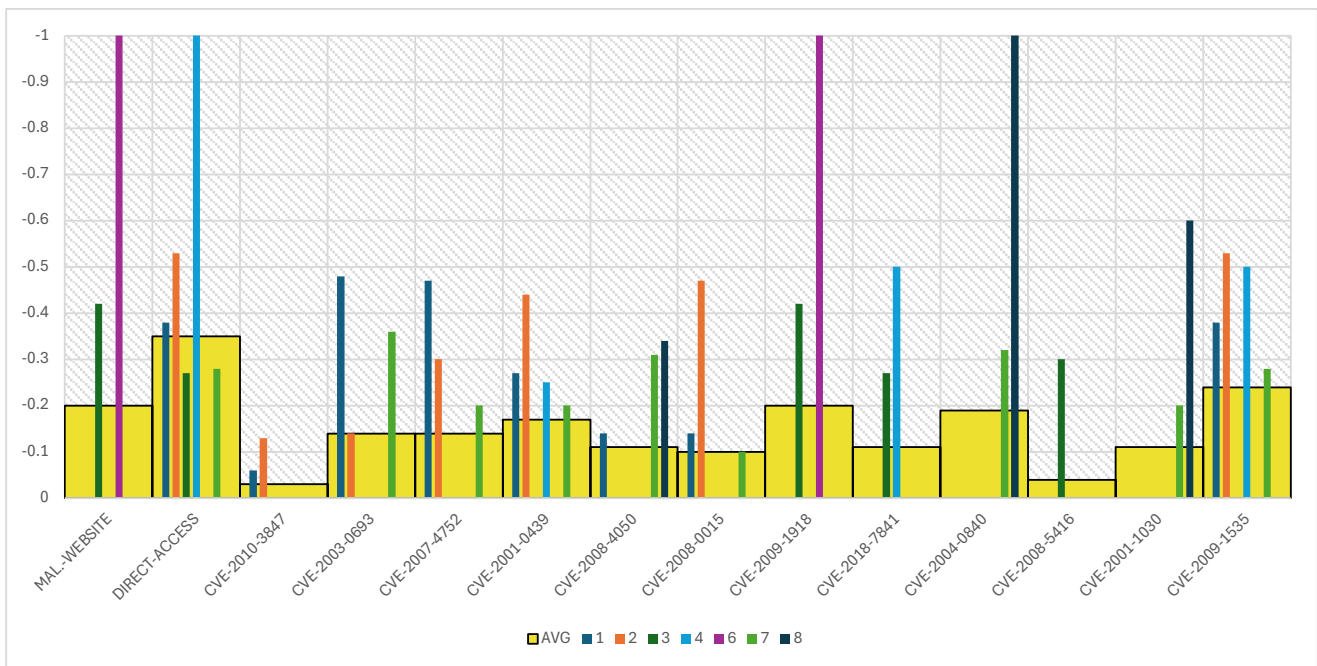


Fig. 7: Relative change in the node-wise expected cumulative outbound impact, C_{OUT} , after fixing a vulnerability. The individual bars represent the relative change of C_{OUT} per node n . Note the reversed vertical axis.

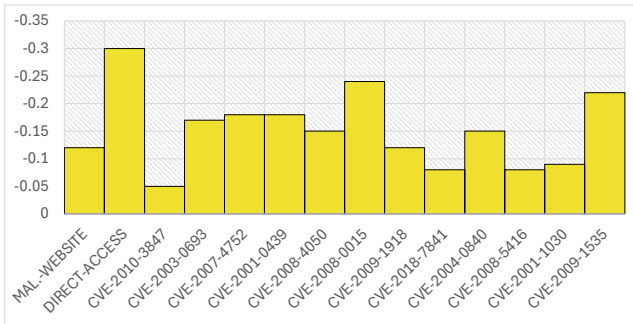


Fig. 8: Relative change in the cumulative impact per attack state, $CE[IS_{18}]$, after fixing a vulnerability. Note the reversed vertical axis.

on the node or of the services running on nodes that can be attacked from it, one node at a time. In these calculations, we assume that adding monitoring to a node would reduce the probability of exploitation of incoming attack vectors to a node or its outgoing attack vectors an attacker could exploit in an attack. That is, the exploitability of the node’s inbound and outbound attack vectors is affected by a common factor f :

$$\hat{p}_E(i, j) = f * p_E(i, j).$$

The internal attack vectors remain unchanged. To demonstrate the effect of added monitoring, we use a factor of $f = 0.2$ in our calculations, which means that the exploitability of each affected vulnerability is reduced by 80%.

The relative changes of the node-wise expected impacts C_{IN} and C_{OUT} are presented in Figures 9 and 10, respectively. The results we obtain are consistent with those acquired from the vulnerability mitigation simulations. It is obvious that adding monitoring to a node mainly affects its own expected cumulative inbound and outbound impacts, with the exception of $C_{IN}(4)$ and $C_{IN}(6)$, which are already zero in the initial case. More interesting is how added monitoring affects the inbound impact of nodes later in the attack path and the outbound impact of nodes both earlier and later in the attack path. In general, adding monitoring to the nodes that are targeted early in the attack (nodes 1, 4, 6, and 8) tends to have higher relative change than adding monitoring to those that are targeted later (i.e., nodes 2, 3, and 7). By adding monitoring to the early states of the attack, the probability of successfully exploiting the early states of the attack without being caught is reduced, and therefore the probability of reaching the latter states is also reduced, which in turn reduces the expected impact of the attack.

Unsurprisingly, adding monitoring to node 4 results in the largest relative change in C_{IN} and C_{OUT} when

averaged over the nodes. This could be expected, as fixing its foothold vulnerability *DIRECT-ACCESS* results in the largest relative change in C_{IN} , C_{OUT} and $CE[IS_{18}]$ in the vulnerability fixing case. Also consistent with the previous findings is that adding monitoring to node 2 results in high relative changes of both C_{IN} and C_{OUT} . This is explained by vulnerabilities affecting node 2, such as *CVE-2008-0015* and *CVE-2001-0439*, both of which have a large change in $CE[IS_{18}]$ in the vulnerability mitigation case.

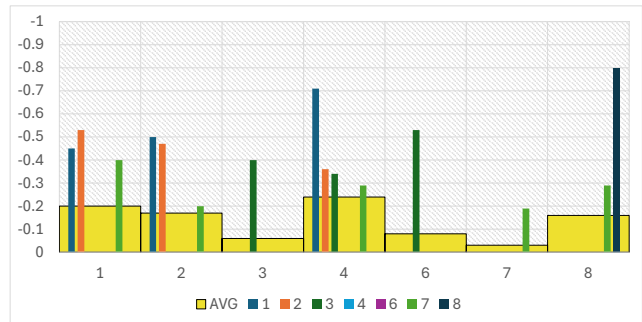


Fig. 9: Relative change in the node-wise expected cumulative inbound impact, C_{IN} , after adding monitoring to a network service. The horizontal axis represent the number of the node with added monitoring. The individual bars represent the relative change of $C_{IN}(n)$ per node n . Note the reversed vertical axis.

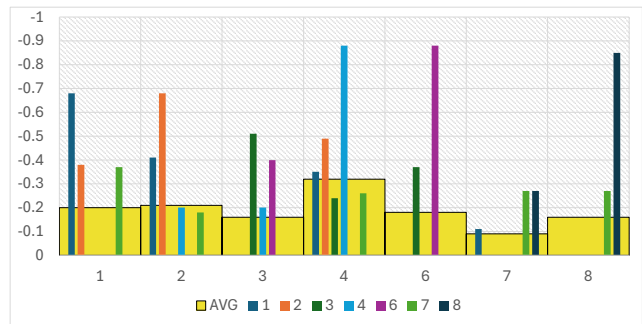


Fig. 10: Relative change in the node-wise expected cumulative outbound impact, C_{OUT} , after adding monitoring to a network service. The horizontal axis represent the number of the node with added monitoring. The individual bars represent the relative change of $C_{OUT}(n)$ per node n . Note the reversed vertical axis.

Figure 11 shows the relative change in the expected cumulative impact of a successful attack ($CE[IS_{18}]$) after adding monitoring to each of the nodes affected by the attack individually. Although these results mainly

conform to the relative change measured by C_{IN} and C_{OUT} , there are some differences. For example, adding monitoring to node 2 reduces the expected cumulative impact the most when analysing the entire attack. While this does not reflect the C_{IN} and C_{OUT} values, it is consistent with the findings of $CE[I_{S18}]$ in the vulnerability mitigation case (see Figure 8), namely high relative changes of vulnerabilities affecting node 2, such as *CVE-2008-0015*. In addition, this can be further explained by the high number of attack paths that exploit the node.

Another clear difference on the scale of the entire attack is the significance of adding monitoring to node 7 compared to the C_{IN} and C_{OUT} cases, in which node 7 could be interpreted as the least significant node in terms of relative change in cumulative impact after added monitoring. When analysing the relative change of adding monitoring to it on the scale of the whole attack, it is equally significant to node 8 and more significant than node 6. This can be explained in a similar way as the factor of the importance of vulnerabilities (such as *CVE-2008-4050*) on $CE[I_{S18}]$ affecting node 7 and the number of attack paths exploiting it.

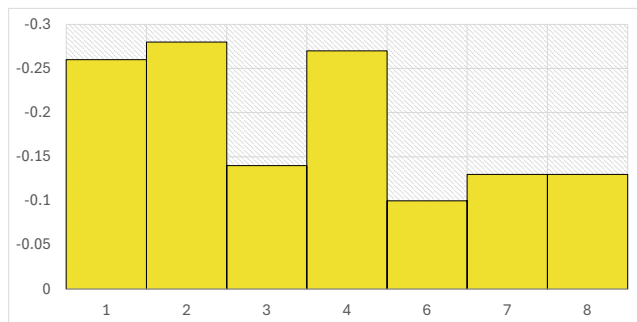


Fig. 11: Relative change in the cumulative impact per attack state, $CE[I_{S18}]$, after adding monitoring to a network service. The horizontal axis represent the number of the node with added monitoring. Note the reversed vertical axis.

4.4 Varying network link weights

So far, we have maintained the weights of the network links at $w_n = 1.0$, which means that the state-to-state probabilities have been $p_N = 1.0$ at the network level. In practice, this means that if the attacker has sufficient skills or other resources (the amount represented by "exploitability"), the attack is always successful. In the attack mitigation and node monitoring scenarios, we only made changes to the relevant attack vector weights

as both scenarios only affected the exploitability of the known vulnerabilities of the services. In the present scenario, we demonstrate how the metrics behave if the underlying weights of the network link weights (w_n) are varied. In real-life use cases, this could be analogous to, for example, adding monitoring of suspicious activity to the entire network, or just simply decreasing network connectivity.

We perform a series of calculations, each after setting all network link weights to a fixed value that we vary between runs ($w_n \in \{0.2, 0.4, 0.6, 0.8, 1.0\}$). The network graph with newly set link weights is combined with the attack graph, and the overall state-to-state probabilities are calculated. Since link weights only affect node-to-node traffic, the probability of successful exploitation of an attack vector is unaffected when the w_n is decreased if the source and target states of an attack vector are in the same node. If, however, they are not, the more node-to-node hops there are between the states, the more the possibility of a successful exploitation decreases due to the p_N in Eq. 1 being dependent on the underlying network link weights. In addition, the fewer possible paths through the network between states, the smaller p_N is. Therefore, in theory, low network link weights favor attack paths that have fewer node-to-node hops and more possible paths between the attack states, but this is not always evident from our results, as our metrics do not focus on individual attack paths.

The attack state-wise expected cumulative impact ($CE[I]$) is presented in Figure 12a. In general, there is a clear trend that the network link weights of $w_n = 0.8$ have a relatively small effect on the cumulative impact compared to the results obtained with the link weights of $w_n = 1.0$. This is explained by the fact that there are multiple possible paths between the network nodes and with a high link weight, the probability of reaching a node from another node still remains relatively high. When the weights are further decreased, this probability decreases rapidly, and there is clearly a larger drop in $CE[I]$ with link weights of $w_n = 0.6$ and $w_n = 0.4$. The rate of change in probability is again more subtle when the weights are further decreased to $w_n = 0.2$, which is indicated by a smaller drop in $CE[I]$.

Since decreasing w_n does not affect the probability of successful exploitation of vulnerabilities that provide access to the network or of vulnerabilities between attack states within the same node, their expected cumulative impact remains unaffected. This can be seen in Figure 12a by comparing the $CE[I_{S5}]$ and $CE[I_{S6}]$ obtained with different network weights. However, if a state can be reached from both a state affected by link weights and a foothold state within the same node, its

$CE[I]$ is affected by the link weights, which is the case for $CE[I_{S8}]$, as $p_N(S12, S8)$ is dependent on w_n .

To understand how the link weights affect the impact of vulnerabilities we repeat the analysis of fixing each vulnerability with varying network link weights and calculate the relative changes in the expected cumulative impact of a successful attack ($CE[I_{S18}]$). As previously established, with low link weights, node-to-node communication becomes less likely. This is clearly reflected in the results presented in Figure 12b, where it is seen that lowering w_n results in an emphasis on mitigating vulnerabilities that can be exploited before there is a hop from node to node in the attack path. For example, if measured by $CE[I_{S18}]$, *CVE-2008-4815* and *CVE-2008-0015* both are among the most important vulnerabilities when w_n is high but amongst the most trivial if w_n is low.

Mitigating vulnerabilities in the early steps of attack path results in higher relative change in $CE[I_{S18}]$ for low w_n and lower change for high w_n , but interestingly, not always. For example, in the case of vulnerability *CVE-2018-7841* in node 4, the relative change tends to be greater the lower the w_n but the opposite is true for *CVE-2009-1535*, which is also a node 4 vulnerability. This is due to the low cumulative impact after exploiting *CVE-2009-1535*, which is caused by the decreased probability of attacking node 3 from node 4 ($p(S13, S4)$). The decreased probability itself can be explained by the crucial role the underlying network plays when attacking from one node to another. Specifically, if $w_n < 1.0$, the more hops there are between two nodes in the network, the less likely an attack between them will succeed. This is not only seen with *CVE-2009-1535*, but especially so with *CVE-2008-5416*, which requires that the attack has already reached node 3. As seen in the attack graph in Figure 3, the only possible ways to attack node 3 are from nodes 4 and 6. However, due to the network structure, which can be seen in Figure 2, node 3 is at minimum three hops away from node 4 or 6, which makes reaching node 3 extremely improbable during an attack, if w_n is low. Fixing a vulnerability beyond this point becomes less significant with low link weights and, if $w_n = 0.2$, fixing *CVE-2008-5416* results in a near-zero relative change of $CE[I_{S18}]$, as demonstrated in Figure 12b.

Analogous to the vulnerability fixing simulation with varying network link weights, we also ran a series of simulations to analyse the role of the network link weights in the scenario, in which we add monitoring to a node for its known vulnerabilities. That is, in each run, we set the network weights to a fixed value, calculated the expected impact of a successful attack and then calculated the relative change of $CE[I_{S18}]$ after adding mon-

itoring for known vulnerabilities to each of the nodes, one at a time.

Similarly to the vulnerability fixing simulation results, with lower link weights, adding monitoring to nodes that are targeted early in the attack tends to have a higher relative change of $CE[I_{S18}]$ than nodes further down the attack paths. This is clearly seen in Figure 12c by looking at the relative change of $CE[I_{S18}]$ after adding monitoring to node 8. Clearly, if the network link weights are lower and the attack from one node to another is less probable, the change is greater than with higher network link weights. The same effect can be seen in Figure 12b by looking at the relative change of $CE[I_{S18}]$ after fixing the vulnerability *CVE-2004-0840*, which provides a foothold into node 8. In contrast, we can see the opposite effect by looking at the results of node 3 that are nearly identical to those of the vulnerability *CVE-2008-5416* in the previous run. The reason for this is that attacking node 3 becomes highly improbable with low network link weights, and thus adding monitoring for attacks exploiting its known vulnerabilities only yields a small relative change of $CE[I_{S18}]$.

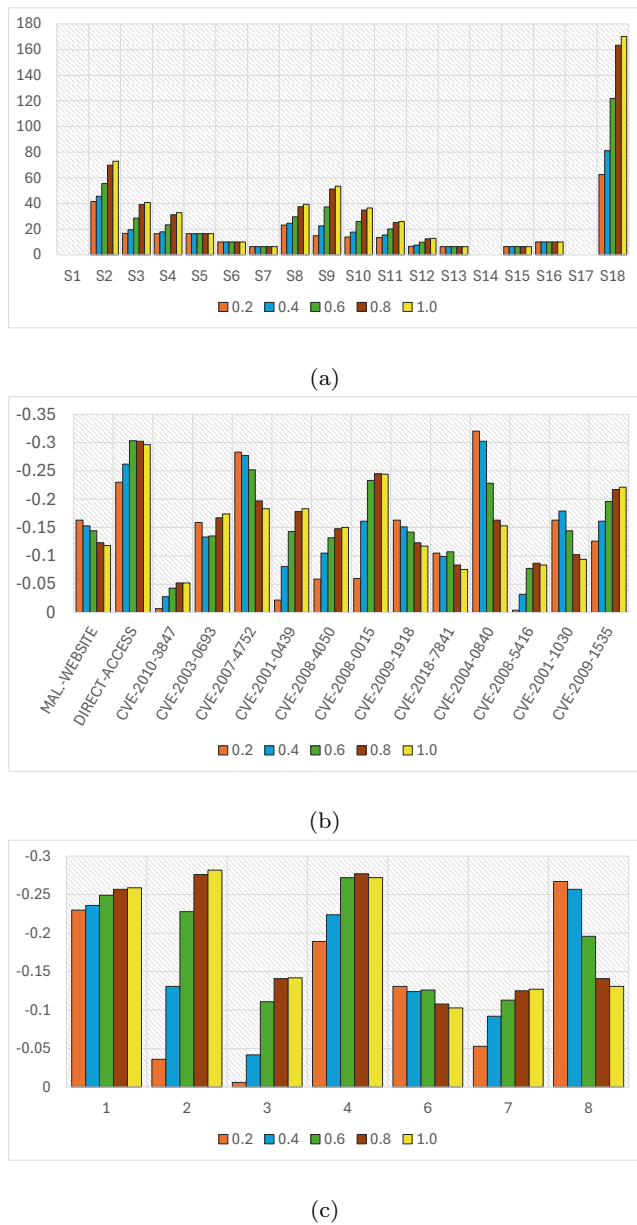


Fig. 12: Influence of varying the network link weights on different impact metrics. In each of the figures, the coloured bars represent the values acquired by setting weight of each network link to a fixed value between 0.2 and 1.0. (a) Attack state-wise expected cumulative impact, $CE[I_i]$. (b) Relative change in the expected cumulative impact of a successful attack ($CE[I_{S18}]$) after fixing a single vulnerability. Note the reversed vertical axis. (c) Relative change in the expected cumulative impact of a successful attack ($CE[I_{S18}]$) after adding monitoring to a network service. Note the reversed vertical axis.

5 Conclusion

In this study, we have presented a novel methodology to model cyber attacks, analyse their paths through exploitable vulnerabilities, and evaluate the impact of cyber exploits on services in an enterprise or infrastructure network. Our model takes into account interconnected dependencies across different network layers, from the physical layer to the application layer. Here, we have employed probabilistic approaches to analyse how cyber attacks propagate through attack graphs and their effects on user services and application layers in communication networks. Our graph-based modelling approach proved to be versatile, as it can be used to investigate cyber threats and attacks at various levels of detail. This methodology also allows the evaluation of different cyber attack scenarios and supports the evaluation of protection and mitigation measures.

In addition, our method for modelling cyber threats and attacks enables the planning and implementation of tailored protective actions, taking into account the importance of services as experienced by users. The proposed methodology helps security specialists and system administrators make well-informed decisions regarding risk mitigation strategies.

Acknowledgements The authors would like to thank Ambrose Kam and Arlanda Johnson for their invaluable and constructive feedback on the methodology, which helped improve the quality of this study.

References

- [1] Yuchong Li and Qinghui Liu. “A comprehensive review study of cyber-attacks and cyber security; Emerging trends and recent developments”. In: *Energy Reports* 7 (2021), pp. 8176–8186. DOI: <https://doi.org/10.1016/j.egy.2021.08.126>.
- [2] Jasmin Wachter. “Graph models for Cybersecurity—A Survey”. In: *arXiv preprint arXiv:2311.10050* (2023). DOI: <https://doi.org/10.48550/arXiv.2311.10050>.
- [3] Christos Smiliotopoulos, Georgios Kambourakis, and Constantinos Kolias. “Detecting lateral movement: A systematic survey”. In: *Heliyon* 10.4 (2024), e26317. ISSN: 2405-8440. DOI: <https://doi.org/10.1016/j.heliyon.2024.e26317>.
- [4] Kengo Zenitani. “Attack graph analysis: an explanatory guide”. In: *Computers & Security* 126 (2023), p. 103081. DOI: <https://doi.org/10.1016/j.cose.2022.103081>.

- [5] Harjinder Singh Lallie, Kurt Debattista, and Jay Bal. “A review of attack graph and attack tree visual syntax in cyber security”. In: *Computer Science Review* 35 (2020), p. 100219. DOI: <https://doi.org/10.1016/j.cosrev.2019.100219>.
- [6] Jianping Zeng et al. “Survey of attack graph analysis methods from the perspective of data and knowledge processing”. In: *Security and Communication Networks* 2019.1 (2019), p. 2031063. DOI: <https://doi.org/10.1155/2019/2031063>.
- [7] Fredrik Löf et al. “An Approach to Network Security Assessment based on Probabilistic Relational Models”. In: *First Workshop on Secure Control Systems (SCS-1)*. 2010.
- [8] Teodor Sommestad, Mathias Ekstedt, and Hannes Holm. “The Cyber Security Modeling Language: A Tool for Assessing the Vulnerability of Enterprise System Architectures”. In: *IEEE Systems Journal* 7.3 (2013), pp. 363–373. DOI: <https://doi.org/10.1109/JSYST.2012.2221853>.
- [9] Richard Lippmann et al. “Validating and restoring defense in depth using attack graphs”. In: *MILCOM 2006-2006 IEEE military communications conference*. IEEE, 2006, pp. 1–10. DOI: <https://doi.org/10.1109/MILCOM.2006.302434>.
- [10] Steven Noel. “A review of graph approaches to network security analytics”. In: *From Database to Cyber Security: Essays Dedicated to Sushil Jajodia on the Occasion of His 70th Birthday* (2018), pp. 300–323. DOI: https://doi.org/10.1007/978-3-030-04834-1_16.
- [11] Sofiane Lagraa et al. “A review on graph-based approaches for network security monitoring and botnet detection”. In: *International Journal of Information Security* 23.1 (2024), pp. 119–140. DOI: <https://doi.org/10.1007/s10207-023-00742-7>.
- [12] Nwokedi Idika and Bharat Bhargava. “Extending attack graph-based security metrics and aggregating their application”. In: *IEEE Transactions on dependable and secure computing* 9.1 (2010), pp. 75–85. DOI: <https://doi.org/10.1109/TDSC.2010.61>.
- [13] Xinming Ou and Anoop Singhal. *Quantitative security risk assessment of enterprise networks*. Springer, 2011. DOI: <https://doi.org/10.1007/978-1-4614-1860-3>.
- [14] George Stergiopoulos, Panagiotis Dedousis, and Dimitris Gritzalis. “Automatic analysis of attack graphs for risk mitigation and prioritization on large-scale and complex networks in Industry 4.0”. In: *International Journal of Information Security* 21.1 (2022), pp. 37–59. DOI: <https://doi.org/10.1007/s10207-020-00533-4>.
- [15] Ayan Gain and Mridul Sankar Barik. “Attack Graph Based Security Metrics for Dynamic Networks”. In: *International Conference on Information Systems Security*. Springer, 2023, pp. 109–128. DOI: https://doi.org/10.1007/978-3-031-49099-6_7.
- [16] Barbara Kordy, Ludovic Piètre-Cambacédès, and Patrick Schweitzer. “DAG-based attack and defense modeling: Don’t miss the forest for the attack trees”. In: *Computer science review* 13 (2014), pp. 1–38. DOI: <https://doi.org/10.1016/j.cosrev.2014.07.001>.
- [17] Xinming Ou and Anoop Singhal. “Security Risk Analysis of Enterprise Networks Using Attack Graphs”. In: *Quantitative Security Risk Assessment of Enterprise Networks*. New York, NY: Springer New York, 2011, pp. 13–23. ISBN: 978-1-4614-1860-3. DOI: https://doi.org/10.1007/978-1-4614-1860-3_4.
- [18] Vesa Kuikka and Kimmo K. Kaski. “Detailed-level modelling of influence spreading on complex networks”. In: *Scientific Reports* 14.28069 (2024). DOI: <https://doi.org/10.1038/s41598-024-79182-9>.
- [19] Pratyusa K. Manadhata and Jeannette M. Wing. “An Attack Surface Metric”. In: *IEEE Transactions on Software Engineering* 37.3 (2011), pp. 371–386. DOI: <https://doi.org/10.1109/TSE.2010.60>.
- [20] Marcel Frigault et al. “Measuring the Overall Network Security by Combining CVSS Scores Based on Attack Graphs and Bayesian Networks”. In: *Network Security Metrics*. Cham: Springer International Publishing, 2017, pp. 1–23. ISBN: 978-3-319-66505-4. DOI: https://doi.org/10.1007/978-3-319-66505-4_1.
- [21] Ginestra Bianconi. *Multilayer networks: structure and function*. Oxford university press, 2018.
- [22] Roberto Interdonato et al. “Multilayer network simplification: approaches, models and methods”. In: *Computer Science Review* 36 (2020), p. 100246. DOI: <https://doi.org/10.1016/j.cosrev.2020.100246>.
- [23] Lingyu Wang, Sushil Jajodia, and Anoop Singhal. *Network security metrics*. Springer, 2017. DOI: <https://doi.org/10.1007/978-3-319-66505-4>.
- [24] John Homer et al. “Aggregating vulnerability metrics in enterprise networks using attack graphs”. In: *Journal of Computer Security* 21.4 (2013), pp. 561–597. DOI: <https://doi.org/10.3233/JCS-130475>.

- [25] Marcus Pendleton et al. “A survey on systems security metrics”. In: *ACM Computing Surveys (CSUR)* 49.4 (2016), pp. 1–35. DOI: <https://doi.org/10.1145/3005714>.
- [26] Peter Mell, Karen Scarfone, and Sasha Romanosky. *A Complete Guide to the Common Vulnerability Scoring System Version 2.0*. en. July 30, 2007. URL: https://tsapps.nist.gov/publication/get_pdf.cfm?pub_id=51198.
- [27] Steven Noel and Sushil Jajodia. “A Suite of Metrics for Network Attack Graph Analytics”. In: *Network Security Metrics*. Cham: Springer International Publishing, 2017, pp. 141–176. ISBN: 978-3-319-66505-4. DOI: https://doi.org/10.1007/978-3-319-66505-4_7.
- [28] M. O. Ball, C. J. Colbourn, and J. S. Provan. “Network reliability.” In: *Handbooks in Operations Research and Management Science. Chapter 11*. 7 (1995), pp. 673–762.
- [29] Vesa Kuikka and Heikki Rantanen. “Resilience of multi-layer communication networks”. In: *Sensors* 23.1 (2022), p. 86. DOI: <https://doi.org/10.3390/s23010086>.
- [30] Into Almiala, Henrik Aalto, and Vesa Kuikka. “Influence spreading model for partial breakthrough effects on complex networks”. In: *Physica A: Statistical Mechanics and its Applications* 630 (2023), p. 129244. DOI: <https://doi.org/10.1016/j.physa.2023.129244>.
- [31] Paul Ammann et al. “A Host-Based Approach to Network Attack Chaining Analysis”. In: *Proceedings of the 21st Annual Computer Security Applications Conference. ACSAC '05*. USA: IEEE Computer Society, 2005, pp. 72–84. ISBN: 0769524613. DOI: <https://doi.org/10.1109/CSAC.2005.6>.
- [32] Steven Noel and Sushil Jajodia. *Proactive intrusion prevention and response via attack graphs*. 2009. URL: https://csis.gmu.edu/noel/pubs/2008_IDS_chapter.pdf.
- [33] Jeffrey Stuckman and James Purtilo. “Comparing and applying attack surface metrics”. In: *Proceedings of the 4th international workshop on Security measurements and metrics*. 2012, pp. 3–6. DOI: <https://doi.org/10.1145/2372225.2372229>.
- [34] Yassine Ayrou, Amine Raji, and Mahmoud Nassar. “Modelling cyber-attacks: a survey study”. In: *Network Security* 2018.3 (2018), pp. 13–19. DOI: [https://doi.org/10.1016/S1353-4858\(18\)30025-4](https://doi.org/10.1016/S1353-4858(18)30025-4).
- [35] Zaynab Hammoud and Frank Kramer. “Multi-layer networks: aspects, implementations, and application in biomedicine”. In: *Big Data Analytics* 5.1 (2020), p. 2. DOI: <https://doi.org/10.1186/s41044-020-00046-0>.
- [36] Jin B Hong and Dong Seong Kim. “Towards scalable security analysis using multi-layered security models”. In: *Journal of Network and Computer Applications* 75 (2016), pp. 156–168. DOI: <https://doi.org/10.1016/j.jnca.2016.08.024>.
- [37] Vesa Kuikka et al. “Efficiency of Algorithms for Computing Influence and Information Spreading on Social Networks”. In: *Algorithms* 15.8 (2022). ISSN: 1999-4893. DOI: 10.3390/a15080262. URL: <https://www.mdpi.com/1999-4893/15/8/262>.
- [38] Ronald Ross. *Guide for Conducting Risk Assessments*. en. Sept. 17, 2012. DOI: <https://doi.org/10.6028/NIST.SP.800-30r1>.
- [39] Vesa Kuikka et al. *Network Modelling in Analysing Cyber-related Graphs*. 2024. arXiv: 2412.14375 [cs.SI]. URL: <https://arxiv.org/abs/2412.14375>.

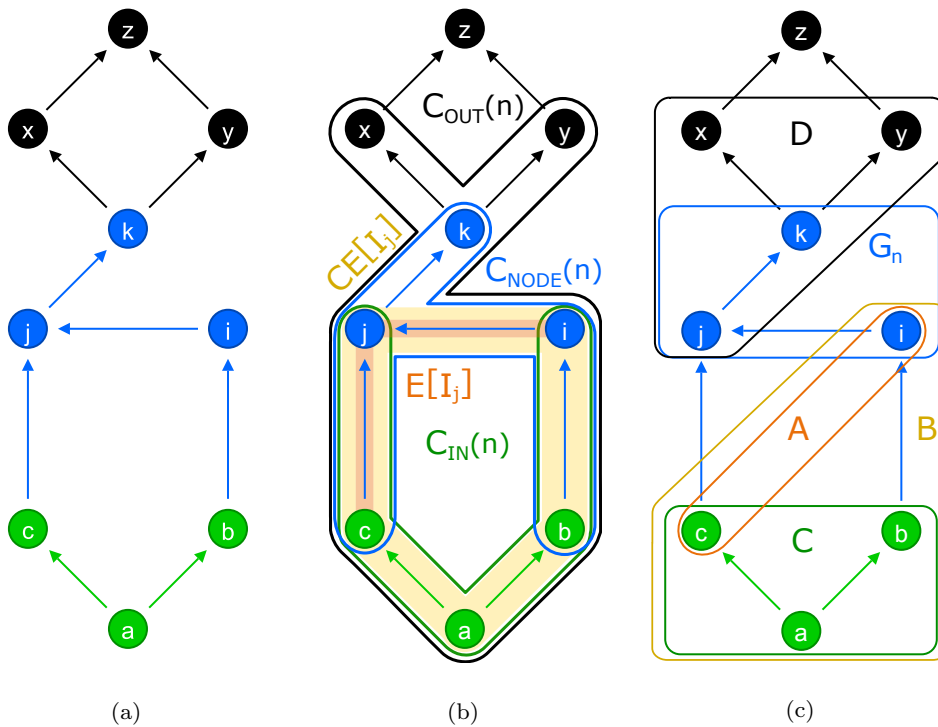


Fig. 13: Visual representation of the utilized metrics and sets used in their equations. Blue states are grouped to node n (G_n), green and black are the states prior to and after G_n on attack paths, respectively. (a) An attack graph. (b) Demonstrated metrics. Coloured lines (node n metrics) and solid colour (state j metrics) indicate the attack vectors, whose impact is included in the corresponding metric. (c) Sets used in the equations of the metrics. Coloured lines indicate the set membership of the attack states. The set's colour matches the metric it belongs to.

Appendix A: Cumulative Metrics Example

An example of a simple attack graph is presented in Figure 13a. It consists of nine attack states with ten attack vectors between them. The states a and z are the start and end states, respectively. In this example, the states i , j and k are grouped to a node n (G_n), as indicated by their blue color. The green states a , b and c precede the G_n states on the attack paths, and the black states x , y , and z come after the G_n states.

Using node n and the attack state j as examples, we show which attack vector impact values are relevant for node-wise metrics $C_{IN}(n)$, $C_{OUT}(n)$ and $C_{NODE}(n)$ (Eq. 4, 5 and 6, respectively), as well as $E[I_j]$ (Eq. 2) and $CE[I_j]$ (Eq. 3) for attack state j . A visual representation of these metrics and their included attack vectors is shown in Figure 13b. To further help explain the metrics, the different sets used in their equations are presented in Figure 13c. In the figures, the colours of the metrics and the colours of the sets in their equations match, although G_n also appears in the equations for $C_{IN}(n)$ and $C_{OUT}(n)$.

The set A is an example of which states are considered to be *immediately* preceding the state j when

calculating $E[j]$ and B is an example of states that are considered to precede the state j on every possible attack path when calculating $CE[I_j]$. The states grouped to node n are represented in set G_n . All the non- G_n states preceding them on any path and any state that can be attacked from them are represented by sets C and D , respectively.

Since the attack vectors ($v_{start,end}$) $v_{b,i}$ and $v_{c,j}$ provide a foothold into the node n , their impact values and those of the attack vectors preceding them are included in $C_{IN}(n)$. The impact of $v(i,j)$ is excluded as this exploit takes place after gaining access to the node. Similarly, for $C_{OUT}(n)$, the impact values of all the attack vectors until states x and y are taken into account. The state z does not immediately follow any G_n state, and is excluded from the set C . Thus, the vectors $v_{x,z}$ and $v_{y,z}$ are not in $C_{OUT}(n)$. Finally, when calculating $C_{NODE}(n)$, the impact values of the attack vectors targeting any of the G_n states are taken into account, including the impact values of any possible attacks between the G_n states.